Simulated Picosecond-laser-generated Surface Acoustic Waves in Nanostructures

Luke Thatcher '22 and Professor Brian Daly; Physics

Introduction

We have run computer simulations of an ultrafast pump-probe laser experiment that generates and detects surface acoustic waves (SAWs) in periodic structures at the nanoscale (see Fig. 1).

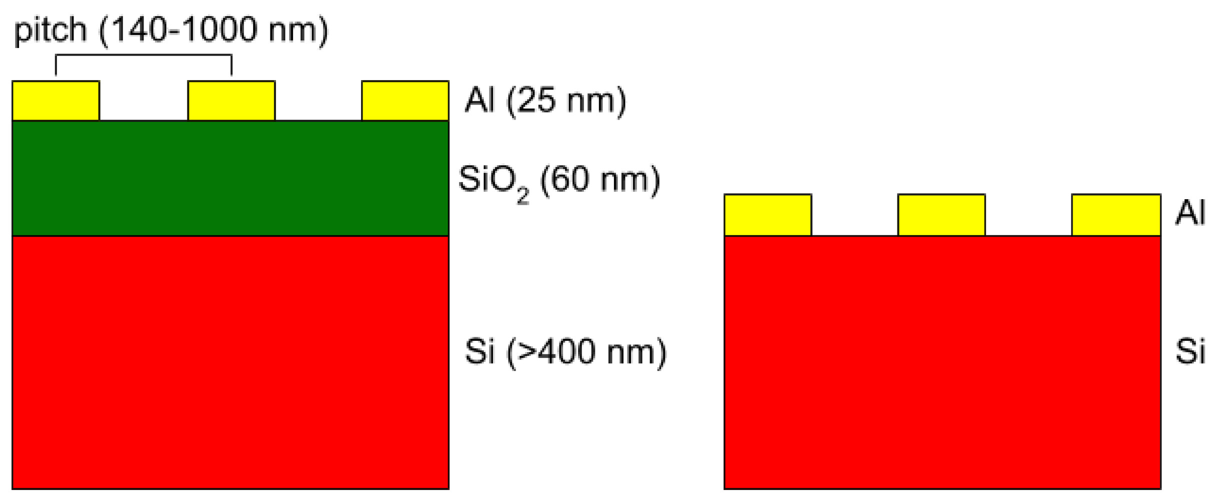

Figure 1: The nanostructures we studied consisted of aluminum bars with various spacing (called 'pitch') on layers of silicon dioxide and silicon. Some structures had no silicon dioxide layer.

In these experiments, a 'pump' beam of light causes strain and generates surface waves in a structure by heating the surface and causing thermal expansion, and a 'probe' beam of light is used to measure the structure's change in reflectivity (see Fig. 2). The change in reflectivity can be used to identify surface waves with frequencies up to 100 GHz (the highest SAW frequencies that can currently be detected). Our simulations consisted of two parts: a mechanical simulation that calculated and showed strains in the structure and allowed us to identify different vibrational modes, and an electromagnetic simulation that used the mechanical strains to simulate changes in the optical reflectivity of the structure. We focused on probe beams of either 400 or 800 nm wavelengths, polarized with the electric field either parallel or perpendicular to the aluminum bars on top of the structures. We sought to find a consistent relationship between vibrational intensity and different wavelength-polarization configurations in different vibrational modes across a variety of nanostructures.

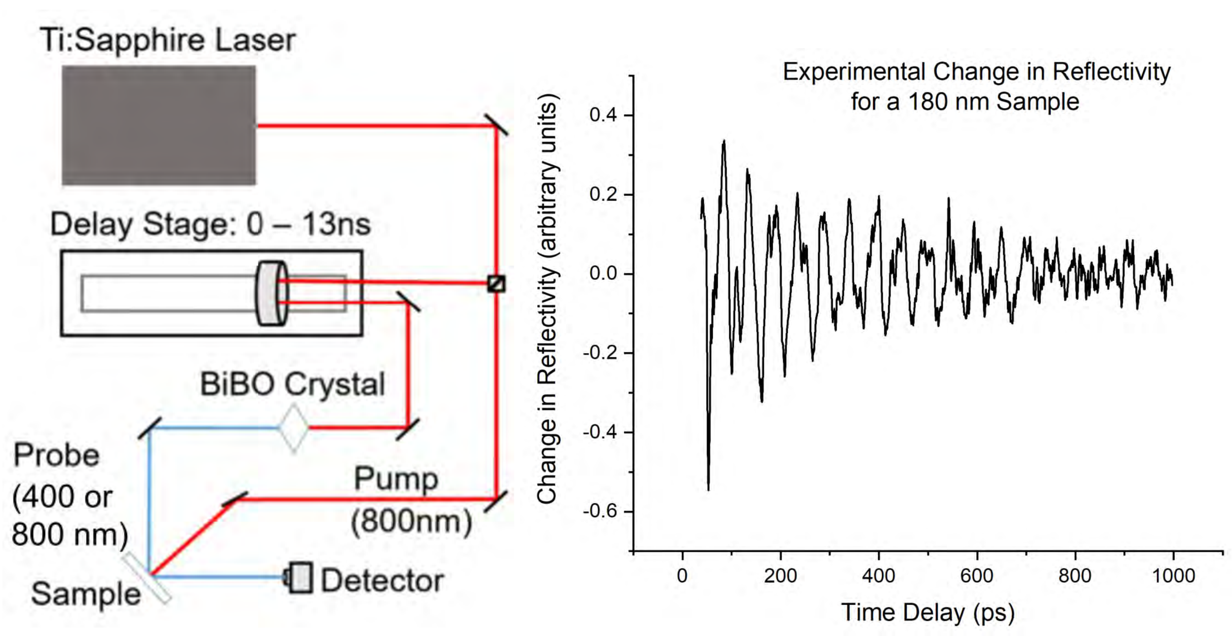

Figure 2: Configuration of the pump-probe laser experiment for generating and detecting SAWs with a Titanium:Sapphire laser (left) and an example of experimental reflectivity data (right).

Methodology

Mechanical Simulation: LayerQuake

To identify SAWs of different vibrational modes, we ran a mechanical simulation called LayerQuake. LayerQuake inputted a two-dimensional drawing of a subsection with only one of the many aluminum bars present on the surface of the sample we wanted to study and used periodic boundary conditions to calculate the two-dimensional strain on the sample as it was heated by a laser. Throughout our simulations, we simulated a laser pulse that exponentially decayed with a time constant of 2 picoseconds. For each sample we studied, we first had LayerQuake output Fourier transforms of the motion of the sample as it was heated by the laser, allowing us to identify the structure's resonant frequencies. We then simulated heating the sample with lasers pulsing at each of these frequencies and generated animations of the vibrations in the structure.

We used these animations to identify three main types of vibrational modes, known as Rayleigh, Sezawa, and bar modes (see Fig. 3).

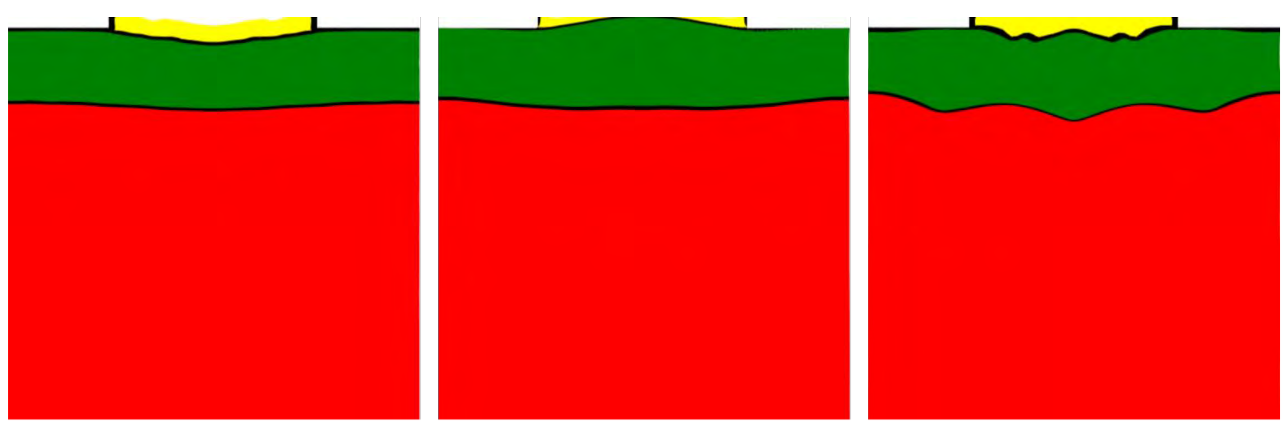

Figure 3: Examples of the three main types of vibrational modes in a 400 nm pitch sample. From left to right: an 11 GHz Rayleigh mode, a 20 GHz Sezawa mode, and a 39 GHz bar mode. Rayleigh modes are characterized by the dioxide layer 'flexing,' while Sezawa modes are characterized by the dioxide layer 'breathing.' Bar modes are resonant frequencies of the aluminum bar, and they produce more complicated vibrations in the dioxide.

Electromagnetic Simulation: FDFD

The reflected probe beam for different polarizations and wavelengths was simulated by an electromagnetic Finite Difference Frequency Domain (FDFD) program which allowed us to calculate reflectivity change versus time due to the strain predicted by LayerQuake. We then took Fourier transforms of the reflectivity calculations from a single laser pulse to identify the frequencies at which the structure vibrated at each configuration of polarization and wavelength. For each sample, we plotted the amplitudes of each frequency spike for the various wavelength-polarization configurations to try to identify patterns in different configurations across different vibrational modes (see Fig. 5).

Results

Figure 4 shows Fourier transforms of the mechanical strain data for four samples that are identical other than the pitch of the aluminum bars. The peaks in each transform predict the frequencies of the vibrational modes of each structure. Structures with smaller pitches tended to have higher frequency modes, although the 200 nm pitch structure had two modes at higher frequencies than the highest frequency mode of the 140 nm pitch structure. In the 400 nm pitch structure, the highest amplitude peak was a Rayleigh mode and the next highest amplitude peak was a Sezawa mode, but in the 140 nm pitch structure, the frequencies corresponding to the first Rayleigh and Sezawa modes had amplitudes that are almost too small to see compared to the amplitude of the 56 GHz bar mode. We found no way of identifying the type of mode from the Fourier amplitudes alone.

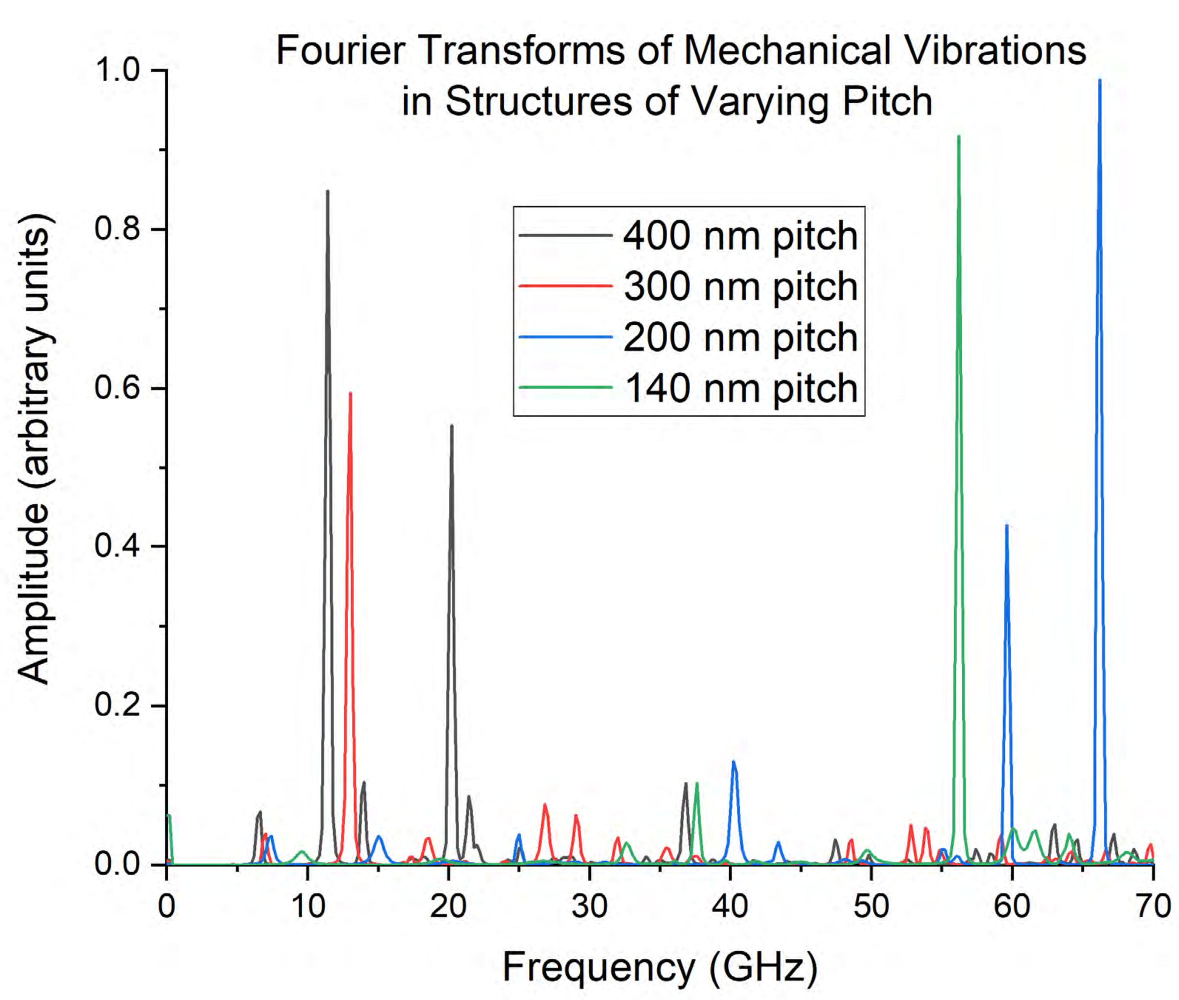

Figure 4: Fourier transforms of the mechanical strain data generated by LayerQuake for samples with aluminum bars of varying pitch.

Figure 5 shows the amplitudes of peaks in the Fourier transforms of the FDFD-generated reflectivity data for a 140 nm sample probed by every combination of either 400 nm or 800 nm wavelength light polarized with the electric field parallel (denoted 'E') or perpendicular (denoted 'H') to the aluminum bars. For the data with a layer of silicon dioxide, there was a consistent relationship between the Fourier amplitude and the various wavelength-polarization configurations at most frequencies. E-polarized light generated stronger vibrations than H-polarized light, and 400 nm wavelength light generated stronger vibrations than 800 nm wavelength light. In the sample without the silicon dioxide, this relationship broke down. The differences in vibrational amplitude between configurations was also not linked with the type of vibrational mode.

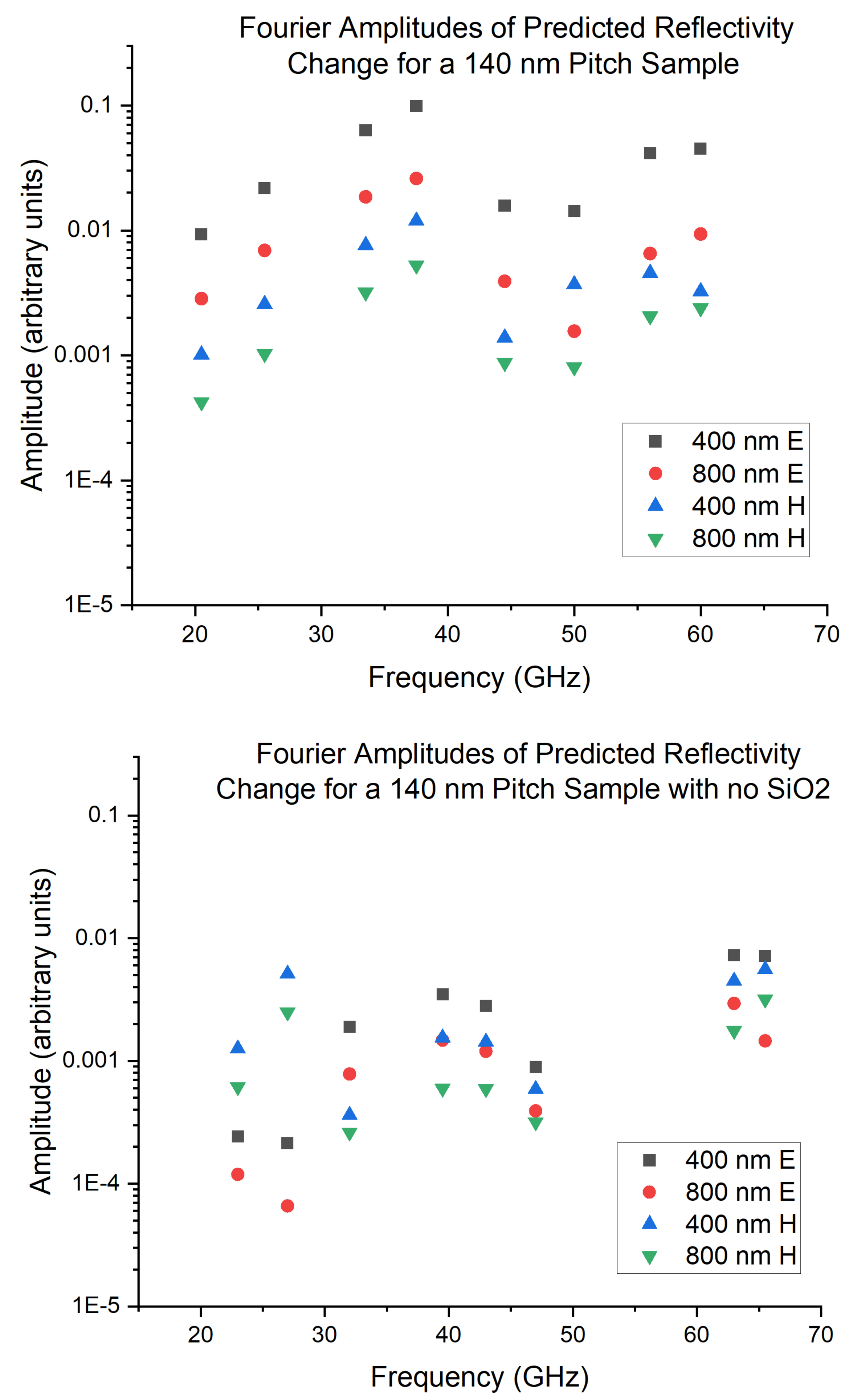

Figure 5: Amplitudes of the strongest frequencies in Fourier transforms of reflectivity data from a sample with 140 nm pitch both with (top) and without (bottom) silicon dioxide.

Conclusion

We were unable to find a consistent relationship between the wavelength-polarization configuration and vibrational intensity and modes in SAWs generated in nanostructures. We were able to demonstrate a mostly consistent order for the Fourier amplitudes of various configurations in a sample with a pitch of 140 nm, but the order varied in samples of different pitches and in samples with and without silicon dioxide, so the vibrational intensity depended on more factors than we initially thought.

References + Acknowledgements

Figure 2 modified from: M. Colletta, W. Gachuhi, B. Daly, "Ultrafast Optical Study of Surface Acoustic Waves on Aluminum Nanostructures", Vassar URSI 2017

We would like to acknowledge and thank the 2020 Vassar URSI program, the generous donation of the Stern Goldin Family Summer Internship Endowment Fund, and NSF Award DMR-1709521.